

Determination of the Interfacial Roughness Exponent in Rare-Earth Superlattices

P. P. Swaddling,¹ D. F. McMorrow,² R. A. Cowley,¹ R. C. C. Ward,¹ and M. R. Wells¹

Oxford Physics, Clarendon Laboratory, Parks Road, Oxford, United Kingdom

Risø National Laboratory, DK-4000 Roskilde, Denmark

(Received 11 March 1994)

The interfacial roughness in Ho/Y and Ho/Lu superlattices has been studied using high-resolution x-ray diffraction. The transverse width of the superlattice Bragg peaks broadens almost linearly as a function of the component of the reduced wave vector parallel to the growth direction, while the line shape is invariant, and is described by a Lorentzian raised to the power of $\approx 5/2$. These results are interpreted as a signature of conformally rough interfaces, and the roughness exponent is determined to be $\alpha = 0.85 \pm 0.05$. It is also shown how α may be altered by adjusting the growth conditions.

PACS numbers: 68.55.Bd, 61.10.Lx, 68.35.Fx

Molecular beam epitaxy (MBE) was originally developed to fabricate semiconductor heterostructures, but is now being used to produce metals, insulators, and even mixed systems [1]. Its great utility results from the relative ease with which it is possible to control the deposition rate and substrate temperature. These determine the balance between fluctuations due to the stochastic nature of the incident beam and surface diffusion and, hence, the growth morphology. In spite of this control it is often difficult to achieve perfect layer-by-layer growth, and instead a rough surface is obtained. A dynamic scaling relation has been proposed for such surfaces, characterized by two exponents α and β that describe the spatial and temporal evolution of the roughness [2]. Although considerable theoretical effort has been devoted to determining the values of these exponents for different growth models, there have been few experimental investigations. In this Letter we report measurements of the diffuse x-ray scattering from a series of MBE-grown rare-earth superlattices, from which we extract the roughness exponent α . In addition, by studying a series of nominally identical samples grown at different substrate temperatures we are able to determine the dependence of the growth morphology on substrate temperature.

In the late-time regime, the dynamic scaling form of the equal-time height-height correlation function $G(r)$ describing a rough surface of area L^2 is given by [2]

$$G(r) = \langle [h(r) - h(0)]^2 \rangle = \begin{cases} Ar^{2\alpha} & \text{for } r \ll L \\ h_0 & \text{for } r \gg L, \end{cases} \quad (1)$$

where $h(r)$ describes the height of the surface as a function of the in-plane position r , $\langle \dots \rangle$ denotes an ensemble average, and A and h_0 are constants. Provided that L is sufficiently large, the diffuse x-ray intensity in the limit $r \ll L$ from a surface described by the correlation function $G(r)$ may be written as [3,4]

$$I(\mathbf{p}, q) \propto \int_0^\infty r \exp(-Aq^2 r^{2\alpha}/2) J_0(pr) dr. \quad (2)$$

Here J_0 is zeroth-order Bessel function, and we write the reduced x-ray wave-vector transfer relative to the main

Bragg peak as (p_x, p_y, q) , with \mathbf{p} in the plane of the film and q perpendicular to the surface. This integral can only be evaluated analytically for two values of the exponent α : if $\alpha = 1/2$, then the transverse line shape is a Lorentzian to the power of $3/2$, with a width that varies quadratically with q , while $\alpha = 1$ yields a Gaussian line shape and a width that varies linearly with q . As the value of α is increased from $1/2$, the line shape can be described as a Lorentzian raised to successively higher powers. Thus, in principle, by measuring how the x-ray scattering evolves as a function of \mathbf{p} and q , it is possible to determine the roughness exponent α . For $r \gg L$, the effect of a constant $G(r)$ is to produce a delta function in the x-ray scattering, so that in general the line shape consists of a diffuse component given by Eq. (2) and a resolution limited Bragg peak. The observed ratio of these two components then depends sensitively on the experimental resolution and may also be affected by factors such as the mosaic distribution of the sample. These arguments have been developed for a surface, but can be generalized to include the interfaces between the two constituents forming a superlattice. In this case, a diffuse component given by Eq. (2) will be observed if the interfacial roughness is conformal, in the sense that it is correlated from one interface to the next.

Models developed to describe the growth process fall into two categories. In the first, it is assumed that relaxation mechanisms, such as surface diffusion, are sufficient to prevent the formation of voids and overhangs. For this conservative growth mode it has been shown that the roughness exponents, and in particular α , are very sensitive to the local rules governing the relaxation, with typical values in $d = 2 + 1$ dimensions spanning the range from $\alpha = 2/3$ [5] to $\alpha = 0.95$ [6]. In contrast, nonconservative growth models are believed to belong to the single Kardar-Parisi-Zhang (KPZ) universality class [7], which for $d = 2 + 1$ predicts that $\alpha = 1/3$. (Here the lower value of α simply reflects the fact that in the absence of strong relaxation processes a more jagged surface is likely to form.) There is still some controversy [8–11] over which, if either, of the above growth modes

correctly describes MBE, and this provided the motivation for our study.

For metallic systems we are only aware of two previous determinations of the spatial roughness exponent: an electron diffraction study of the growth of Fe on Fe (001) yielded $\alpha = 0.79 \pm 0.05$ [12], and low-angle x-ray scattering measurements of Co/Pt superlattices gave $\alpha = 0.65 \pm 0.03$ [13]. Other systems investigated using low-angle x-ray scattering include liquid-crystal polymers and semiconductor superlattices, with exponents of 0.25 ± 0.05 [14] and 0.4 [15], respectively.

The rare-earth superlattices were grown using MBE and were originally produced for studies of their magnetic properties. Following the technique developed by Kwo *et al.* [16], the rare-earth metals were deposited on a Nb buffer layer grown on a sapphire substrate (see Refs. [17,18] for more details). In Table I we list their average structural parameters, where we have used the notation $(\text{Ho}_{n_1}/\text{R}_{n_2})_m$, with n_1 and n_2 the numbers of atomic planes, m is the number of bilayers, and $R = \text{Y or Lu}$. All of the superlattices listed in Table I were grown at a nominal substrate temperature of 300°C . It should be noted, however, that they were grown on different occasions over a period of two years, during which time several adjustments were made to the MBE chamber, with the result that it is difficult to compare the absolute values of the quoted substrate temperatures. To overcome this problem, and in particular to allow us to investigate any dependence of the interface roughness on substrate temperature, a series of three superlattices with nominal composition $(\text{Ho}_{40}/\text{Y}_{15})_{15}$ were produced sequentially with substrate temperatures of 250 , 400 , and 600°C .

The x-ray scattering experiments were performed mainly using a triple-crystal x-ray diffractometer in the Clarendon Laboratory, Oxford University. Additional

measurements were also made using a similar instrument on beam line X22B at NSLS, Brookhaven National Laboratory. In both cases the resolution in the scattering plane was typically 0.001 \AA^{-1} , while the out-of-plane resolution was worse by a factor of approximately 100. For each of the samples studied a scan of the x-ray wave-vector transfer \mathbf{Q} was performed parallel to the growth direction ($[00l]$) in order to ascertain the exact position of the superlattice satellite peaks around the (002). Transverse scans parallel to $[100]$, or p_x in the notation of Eq. (2), were then made through each of the satellites, including a scan through the central peak to determine the sample mosaic distribution function. An attempt was also made to study the diffuse scattering in the reflectivity at low angles. However, these measurements were dominated by the scattering from the very rough oxide on top of the Y capping layer. As the oxide is polycrystalline, it did not affect our data taken at high angle. This study thus demonstrates that it is possible to obtain information on the interfaces using high-angle diffraction, which not only reduces the sensitivity to oxidized overlayers, but also avoids complications arising from dynamical diffraction effects at low angle [3].

As a representative data set, we show in Fig. 1 a series of transverse scans through the superlattice reflections around 002 from sample $\text{Ho}_{16}/\text{Y}_{61}$. (Here we are using the notation that the n th order satellite is displaced a distance in reciprocal space $2\pi n/\Delta$, where Δ is the superlattice period in \AA .) Attempts were made to fit the unusual line shape of the scattering with a single peak function. The best description of the data was found using a Lorentzian raised to the power of $5/2$, which we write as

$$I(p_x) = \frac{I_0}{[1 + (\frac{p_x}{\kappa})^2]^{5/2}}, \quad (3)$$

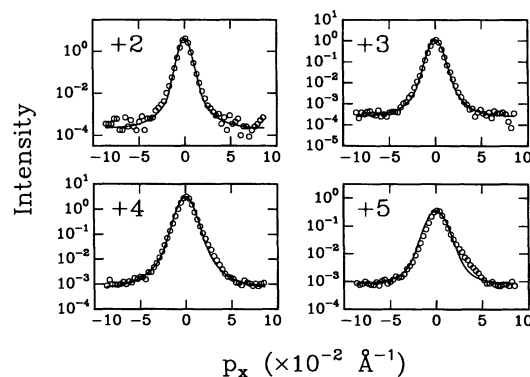


FIG. 1. The x-ray scattering observed in transverse scans through four superlattice satellites of $\text{Ho}_{16}/\text{Y}_{61}$. The solid line represents the result of a simultaneous least-squares fit of Eq. (2), convoluted over the mosaic distribution of the sample and the out-of-plane resolution. The values of the roughness amplitude A and exponent α derived from this fit are given in Table I.

TABLE I. The roughness amplitude A and exponent α determined from modeling the transverse Bragg peak line shapes of Ho/Lu and Ho/Y superlattices. For $\text{Ho}_{16}/\text{Y}_{61}$ two values are given for these parameters corresponding to two orthogonal orientations of the sample around the surface normal; the measured substrate offcut angle is given in parentheses. We estimate that the uncertainty in the value of α is ± 0.05 .

Sample	Amplitude A	Exponent α
$(\text{Ho}_{44}/\text{Lu}_{16})_{50}$	0.020	0.95
$(\text{Ho}_{20}/\text{Lu}_{17})_{50}$	0.049	0.85
$(\text{Ho}_8/\text{Lu}_{18})_{75}$	0.019	0.87
$(\text{Ho}_{18}/\text{Lu}_{10})_{50}$	0.044	0.79
$(\text{Ho}_{12}/\text{Lu}_{34})_{32}$	0.037	0.86
$(\text{Ho}_{18}/\text{Lu}_5)_{50}$	0.034	0.83
$(\text{Ho}_{24}/\text{Lu}_{14})_{50}$	0.050	0.78
$(\text{Ho}_{16}/\text{Y}_{61})_{50} (0.8^\circ)$	0.012	0.89
$(\text{Ho}_{16}/\text{Y}_{61})_{50} (0.1^\circ)$	0.002	0.86
$(\text{Ho}_8/\text{Y}_{30})_{30}$	0.028	0.81

where I_0 is the amplitude and FWHM is related to the inverse correlation length κ by $\text{FWHM} = 1.131\kappa$. The widths (FWHM) of the scattering as a function of n extracted from such fits are displayed in Fig. 2, where it can be seen that they are approximately proportional to the index n and, hence, to the reduced wave vector q parallel to the growth direction. To investigate whether the line shape was isotropic in the plane of the film, we rotated the sample by 90° around [001] and repeated the same scans. The line shape itself was found to be insensitive to orientation, but the widths showed a pronounced anisotropy (Fig. 2). As a final check we also measured the broadening of the superlattice reflections around the 004 peak. It is evident in Fig. 2 that, for a given orientation of the sample, the satellites around the 002 and 004 peaks broaden at the same rate as a function of q . Less exhaustive scattering experiments were performed on all of the superlattices listed in Table I, and yielded qualitatively similar results: the peaks broadened approximately linearly with q , and had a line shape that followed closely a Lorentzian to the $5/2$. (The sole exception to this was sample $\text{Ho}_{44}/\text{Lu}_{16}$, which had a two-component line shape and will be discussed at length elsewhere.)

On the basis of Eq. (2) it would appear that the interfaces in the rare-earth superlattices are rough with a value of the roughness exponent α between $1/2$ and 1 . The fact that a single-component line shape is observed instead of the sum of a diffuse and resolution limited peak may be attributed to the mosaic distribution of the sample, which was typically 0.25° . This removes any sensitivity of the data to the length scales longer than $\approx 150 \text{ \AA}$, thus precluding any estimation of the cutoff length, the distance after which the roughness saturates. To allow a simultaneous analysis of the line shape and its dependence on q we performed a two-dimensional convolution of Eq. (2) over the approximately Gaussian mosaic distribution of the sample and the out-of-plane resolution of the instrument. A least-squares fit was then performed, comparing the model function to all of the transverse scans from one sample to determine the

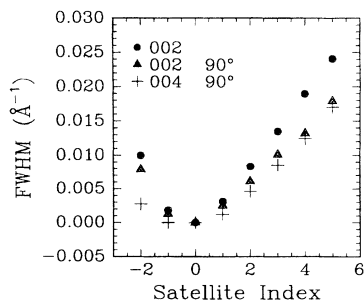


FIG. 2. The measured increase in the width (FWHM) of the superlattice satellite reflections of $\text{Ho}_{16}/\text{Y}_{61}$ around 002 [mounted in the $(h0l)$ plane and rotated by 90°] and 004 as a function of satellite index.

values of α and A . Apart from a background, the only parameter that was allowed to vary between different scans from the same sample was the intensity of each peak which is affected by other factors such as the degree of interdiffusion. The solid lines through the data points in Fig. 1 represent the results of this fitting procedure. It can be seen that the model provides an excellent description of the data, both as a function of wave-vector transfer and satellite index. The value of α extracted for each of the superlattices investigated is given in Table I, and has an average of 0.85 ± 0.05 . For $\text{Ho}_{16}/\text{Y}_{61}$ two sets of values of the fit parameters are quoted for the two orientations of the sample investigated, along with the corresponding measured offcut angle of the sapphire substrate. There is a marked correlation between the magnitude of the offcut angle, which can be directly related to the terrace length on the substrate (see, for example, Ref. [19]), and the roughness: the orientation with the largest offcut, and hence the smallest terraces, produces a rougher interface.

The final set of experiments studied the effect of altering the growth conditions on the interfacial roughness. It has been proposed [20] that fabrication of high-quality metallic superlattices, which is determined by the relative magnitudes of surface diffusion and bulk interdiffusion, requires a growth temperature T_G that is given by $T_G \approx 3/8T_M$, where T_M is the melting temperature of the component metal. (For Ho, Y, and Lu, T_M is, respectively, 1474 , 1522 , and 1663°C .) Here we will restrict ourselves to a consideration of the dependence of the interfacial roughness on T_G only. In Fig. 3 we give a comparison of the observed line shape of the first superlattice satellite from three nominally identical samples grown at different substrate temperatures. As the substrate temperature is decreased there is a striking systematic trend for the width of the peak to broaden. By fitting the profiles using the method outlined above, the observed changes in the line shape, as the substrate temperature is decreased, correspond to an increase in the amplitude A from 0.008 to 0.019 and a concomitant increase in α from 0.83 to 0.93 , as given in Table II. This is a very clear demonstration of the role of substrate temperature in determining

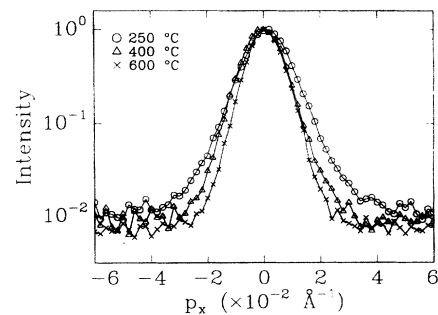


FIG. 3. The dependence of the line shape of the first superlattice satellite on the substrate temperature for three superlattices of nominal structure $(\text{Ho}_{40}/\text{Y}_{15})_{15}$.

TABLE II. The dependence of the roughness amplitude A and exponent α on substrate temperature for a series of $(\text{Ho}_{40}/\text{Y}_{15})_{15}$ superlattices.

Growth temperature (°C)	Amplitude A	Exponent α
250	0.019	0.93
400	0.022	0.87
600	0.008	0.83

the interfacial morphology. As the substrate temperature is reduced atomic surface mobility becomes increasingly restricted. The ability to find sites of high coordination number is limited and the interface roughness increases.

In summary, we have performed a detailed and comprehensive study of the morphology of the interfaces in rare-earth superlattices. From an analysis of the transverse line shape of the superlattice reflections we determine the roughness exponent to be 0.85 ± 0.05 . We believe that this value indicates a conservative growth mode. Because of uncertainties in current theories it is not possible at this stage to draw any further conclusions from its value. We have also demonstrated that x-ray scattering does provide reliable information on the interfacial roughness in MBE growth, and we suggest that the roughness exponent depends on the growth parameters, at least for length scales up to $\approx 150 \text{ \AA}$.

We would like to thank Doon Gibbs for his assistance with the experiments, and Robert Fiedenhans'1 and S.K. Sinha for useful discussions. Beam line X22 is supported by the US DOE under Contract No. DE-AC0276CH00016. This work was supported by a grant from the Science and Engineering Research Council.

[1] Ernst G. Bauer *et al.*, *J. Mater. Res.* **5**, 852 (1990).

- [2] Fereydoon Family, *Physica (Amsterdam)* **168A**, 561 (1990).
- [3] S.K. Sinha, E.B. Sirota, S. Garoff, and H.B. Stanely, *Phys. Rev. B* **38**, 2297 (1988).
- [4] R.A. Cowley, in *Equilibrium Structure and Properties of Surfaces and Interfaces*, edited by A. Gonis and G.M. Stocks (Plenum Press, New York, 1992).
- [5] D. Wolf and J. Villain, *Europhys. Lett.* **13**, 389 (1990).
- [6] S. Das Sarma and S.V. Ghaisas, *Phys. Rev. Lett.* **69**, 3762 (1992).
- [7] M. Kardar, G. Parisi, and Y.C. Zhang, *Phys. Rev. Lett.* **56**, 889 (1986).
- [8] S. Das Sarma and P. Tamborenea, *Phys. Rev. Lett.* **66**, 325 (1991).
- [9] Z.W. Lai and S. Das Sarma, *Phys. Rev. Lett.* **66**, 2348 (1991).
- [10] Hong Yan, *Phys. Rev. Lett.* **68**, 3048 (1992).
- [11] David A. Kessler, Herbert Levine, and Leonard M. Sander, *Phys. Rev. Lett.* **69**, 100 (1992).
- [12] Y.L. He, H.N. Yang, T.M. Lu, and G.G. Wang, *Phys. Rev. Lett.* **69**, 3770 (1992).
- [13] X. Yan and T. Egami, *Phys. Rev. B* **47**, 2362 (1993).
- [14] R.E. Geer, R. Shashidhar, A.F. Thibodeaux, and R.S. Duran, *Phys. Rev. Lett.* **71**, 1391 (1993).
- [15] M.K. Sanyal, S.K. Sinha, A. Gibaud, S.K. Satija, C.F. Majkrzak, and H. Homa, in *Surface X-Ray and Neutron Scattering*, edited by H. Zabel and I.K. Robinson (Springer-Verlag, Berlin, 1992).
- [16] J. Kwo, E.M. Gyorgy, D.B. McWhan, F.J. Disalvo, C. Vettier, and J.E. Bower, *Phys. Rev. Lett.* **55**, 1402 (1985).
- [17] D.A. Jehan, D.F. McMorrow, R.A. Cowley, M.R. Wells, R.C.C. Ward, N. Hagman, and K.N. Clausen, *Phys. Rev. B* **48**, 5594 (1993).
- [18] P.P. Swaddling, D.F. McMorrow, J.A. Simpson, M.R. Wells, R.C.C. Ward, and K.N. Clausen, *J. Phys. Condens. Matter* **5**, L481 (1993).
- [19] A. Gibaud, R.A. Cowley, D.F. McMorrow, R.C.C. Ward, and M.R. Wells, *Phys. Rev. B* **48**, 14463 (1994).
- [20] C.P. Flynn, *J. Phys. F* **18**, L195 (1988).